

# Anomalous-Hall heat current and Nernst effect in the ferromagnet $\text{CuCr}_2\text{Se}_{4-x}\text{Br}_x$ .<sup>\*</sup>

Wei-Li Lee<sup>1</sup>, S. Watauchi<sup>2,\*</sup>, V. L. Miller<sup>2</sup>, R. J. Cava<sup>2</sup>, and N. P. Ong<sup>1</sup>

*Departments of Physics<sup>1</sup> and Chemistry<sup>2</sup>, Princeton University, New Jersey 08544, U.S.A.*

(Dated: September 17, 2018)

In a ferromagnet, an anomalous-Hall heat current, given by the off-diagonal Peltier term  $\alpha_{xy}$ , accompanies the anomalous Hall current. By combining Nernst, thermopower and Hall experiments, we have measured how  $\alpha_{xy}$  varies with hole density and lifetime  $\tau$  in  $\text{CuCr}_2\text{Se}_{4-x}\text{Br}_x$ . At low temperatures  $T$ , we find that  $\alpha_{xy}$  is independent of  $\tau$ , consistent with anomalous-velocity theories. Its magnitude is fixed by a microscopic geometric area  $\mathcal{A} \sim 34 \text{ \AA}^2$ . Our results are incompatible with some models of the Nernst effect in ferromagnets.

PACS numbers: 72.15.Gd, 72.15.Jf, 75.47.-m, 72.10.Bg

In a ferromagnet, the anomalous Hall effect (AHE) is the appearance of a spontaneous Hall current flowing parallel to  $\mathbf{E} \times \mathbf{M}$  where  $\mathbf{E}$  is the electric field and  $\mathbf{M}$  the magnetization [1]. Karplus and Luttinger (KL) [2] proposed that the AHE current originates from an anomalous velocity term which is non-vanishing in a ferromagnet. The topological nature of the KL theory has been of considerable interest recently [3, 4, 5, 6]. Experimentally, strong evidence for the dissipationless nature of the AHE current has been obtained in the spinel ferromagnet  $\text{CuCr}_2\text{Se}_{4-x}\text{Br}_x$ . Lee *et al.* [8] reported that, despite a 1000-fold increase in the resistivity  $\rho$  induced by varying the Br content  $x$ , the anomalous Hall conductivity (normalized per carrier and measured at 5 K) stays at the same value, in agreement with KL's prediction. A test of the anomalous velocity theory against the AHE in Fe has also been reported [7].

It has long been known that an anomalous heat current density  $\mathbf{J}^Q$  also accompanies the AHE current in the absence of any temperature gradient [9, 10]. In principle,  $\mathbf{J}^Q$  can provide further information on the origin of the AHE, but almost nothing is known about its properties. A weak heat current is a challenge to measure. Instead, one often performs the 'reciprocal' Nernst experiment in which a temperature gradient  $-\nabla T$  produces a transverse charge current, which is detected as a Nernst electric field  $\mathbf{E}_N$  parallel to  $\mathbf{M} \times (-\nabla T)$ . However, in previous Nernst experiments on ferromagnets [9, 10, 11],  $\mathbf{J}^Q$  was not found because other transport quantities were not measured. Combining the Nernst signal with the AHE resistivity  $\rho'_{xy}$  and the thermopower, we have determined how the transport quantity  $\alpha_{xy}$  relevant to  $\mathbf{J}^Q$  varies in  $\text{CuCr}_2\text{Se}_{4-x}\text{Br}_x$  as the hole density  $n_h$  and carrier lifetime  $\tau$  are greatly changed under doping. We show that  $\alpha_{xy}$  has a strikingly simple form, with its magnitude scaled by a microscopic geometric area  $\mathcal{A}$ .

We apply a gradient  $-\nabla T \parallel \hat{\mathbf{x}}$  to an electrically-isolated sample in a magnetic field  $\mathbf{H} \parallel \hat{\mathbf{z}}$ . Along  $\hat{\mathbf{x}}$ , the charge current driven by  $-\nabla T$  is balanced by a backflow current

produced by a large  $E_x$  which is detected as the thermopower  $S = E_x/|\nabla T|$ . Along the transverse direction  $\hat{\mathbf{y}}$ , however, both  $E_x$  and  $-\nabla T$  generate Hall-type currents. In general, the charge current in the presence of  $\mathbf{E}$  and  $-\nabla T$  is  $\mathbf{J} = \boldsymbol{\sigma} \cdot \mathbf{E} + \boldsymbol{\alpha} \cdot (-\nabla T)$  with  $\boldsymbol{\sigma}$  and  $\boldsymbol{\alpha}$  the electrical and thermoelectric ('Peltier') conductivity tensors, respectively. Setting  $J_y = 0$ , we obtain the Nernst signal  $e_N \equiv E_y/|\nabla T| = \rho\alpha_{xy} + \rho_{xy}\alpha$  where  $\alpha \equiv \alpha_{xx}$  [12]. Hence, as noted, the Nernst signal results from the 2 distinct  $y$ -axis currents  $\alpha_{yx}(-\nabla T)$  and  $\sigma_{yx}E_x$ . In a ferromagnet, the former is our desired gradient-driven current, whereas the latter comprises the 'dissipationless' AHE current and the weak ordinary Hall current.

In terms of the thermopower  $S = \rho\alpha$  and Hall angle  $\tan\theta_H = \rho_{yx}/\rho$ , we may express  $\alpha_{xy}$  as

$$\rho\alpha_{xy} = e_N + S \tan\theta_H. \quad (1)$$

Hence, to find  $\alpha_{xy}$ , we need to measure  $e_N$ ,  $S$ ,  $\rho_{xy}$  and  $\rho$ . Knowing  $\alpha_{xy}$ , we readily find the transverse heat current  $J_y^Q = \tilde{\alpha}_{yx}E_x$  since  $\tilde{\alpha}_{yx} = \alpha_{yx}T$  by Onsager reciprocity.

The spinel  $\text{CuCr}_2\text{Se}_4$  is a conducting ferromagnet with a Curie temperature  $T_C \sim 450 \text{ K}$ . Because the exchange between local moments in Cr is mediated by superexchange through  $90^\circ$  Cr-Se-Cr bonds rather than the carriers,  $T_C$  is not significantly reduced even when the hole population  $n_h$  drops by a factor of 30 under Br doping ( $M$  at 5 K actually increases by 20%) [8, 13]. Using iodine vapor transport, we have grown crystals with  $x$  from 0.0 to 1.0. As  $x$  increases from 0 to 1, the value of  $\rho$  at 5 K increases by  $\sim 10^3$ , while  $\rho'_{xy}/n_h$  increases by  $\sim 10^6$  [8]. The tunability of  $n_h$  and the robustness of  $M$  under doping make this system attractive for studying charge transport in a lattice with broken time-reversal symmetry. The behavior of  $\rho$ ,  $M$ , and  $\rho'_{xy}$  vs.  $x$  are described in Ref. [8].

Figure 1 shows profiles of  $e_N$  vs.  $H$  at selected  $T$  in 2 samples with  $x = 0.1$  and  $0.85$  and  $T_C = 400$  and  $275 \text{ K}$ , respectively. As noted above,  $e_N(T, H)$  is the sum of two terms both of which scale as  $M$ . The magnitude  $|e_N|$  initially increases as  $H$  rotates domains into alignment and then saturates to a constant for  $H > H_s$ , the saturation field. The sign of  $e_N$  – negative in all samples – reflects the sign of the dominant term [14].

<sup>\*</sup>Phys. Rev. Lett. **93**, 226601 (2004),

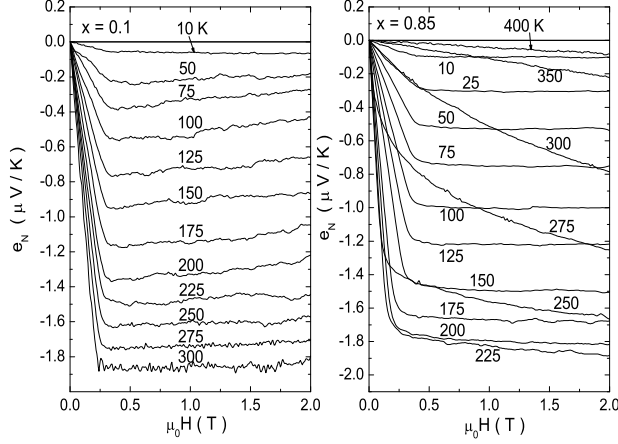


FIG. 1: Curves of the measured  $e_N = E_y/|\nabla T|$  vs.  $H$  in  $\text{CuCr}_2\text{Se}_{4-x}\text{Br}_x$  with  $x = 0.1$  (left panel) and  $0.85$  (right). In the ferromagnetic state below  $T_C$ ,  $e_N$  saturates to a constant when  $H$  exceeds  $H_s$  reflecting the  $M$ - $H$  curve. The scaling factor  $Q_s$  increases rapidly as  $T$  increases from 10 K to  $T_C$ . In the right panel,  $e_N$  continues to scale as the  $M$ - $H$  curve in the paramagnetic regime (275-400 K).

In the sample with  $x = 0.85$ , the curves above  $T_C$  show that the scaling also holds in the paramagnetic regime where the susceptibility has the Curie-Weiss form  $\chi \sim 1/(T - T_C)$  in weak  $H$ . In analogy with the Hall resistivity  $\rho_{xy} = R_0\mu_0 H + R_s\mu_0 M$ , with  $R_0$  and  $R_s$  the ordinary and anomalous Hall coefficients, respectively, it is customary to express the scaling between the  $e_N$ - $H$  and  $M$ - $H$  curves by writing

$$e_N = Q_0\mu_0 H + Q_s\mu_0 M. \quad (2)$$

For  $T < T_C$  in all samples, the  $Q_0$  term cannot be resolved, so that  $e_N \simeq Q_s\mu_0 M$ . Moreover, below 50 K,  $M$  changes only weakly with  $x$  (by 20% over the whole doping range), so that the saturated value of the Nernst signal  $e_N^{\text{sat}}$  differs from  $Q_s$  by a factor that is only weakly  $x$  dependent.

The Nernst signal has very different characteristic behaviors below and above  $T_C$ . As an example, Fig. 2 shows  $e_N^{\text{sat}}$  measured at 2 T in the sample with  $x = 1.0$  ( $T_C = 210$  K). Between 5 and 100 K,  $e_N^{\text{sat}}$  increases linearly with  $T$ . Above 100 K,  $e_N^{\text{sat}}$  rises more steeply to a sharp peak 200 K, and then falls steeply above  $T_C$ . As noted, in the paramagnetic regime, the Nernst signal matches the behavior of  $M$  as a function of both  $T$  and  $H$ . Figure 2 shows that the  $T$  dependence of  $e_N$  closely follows that of  $M = \chi H$  (both are measured at 2 T). The experiment shows that, in a gradient, fluctuations of the paramagnetic magnetization lead to a significant transverse electrical current that is proportional to the average magnetization (this has not been noted before,

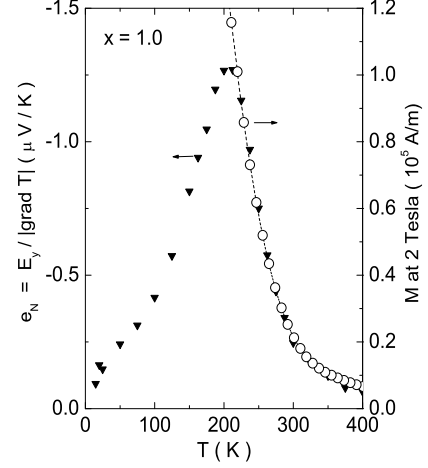


FIG. 2: The  $T$  dependence of the Nernst signal  $e_N$  (solid triangles) measured at 2 T in the sample with  $x = 1.0$ . Above  $T_C$ ,  $e_N$  is compared with the paramagnetic magnetization  $M$  at 2 T (open circles).

to our knowledge). We express the proportionality as

$$\alpha_{xy} = \beta M \quad (T > T_C), \quad (3)$$

where  $\beta$  is only weakly  $T$  dependent (it decreases by 5% between 250 and 400 K). The parameter  $\beta$  plays the important role of relating the magnitudes of the paramagnetic  $M$  and the transverse electronic current (through the Nernst signal). Its very small value ( $\beta \simeq 2 \times 10^{-7} \text{ K}^{-1}$  at 250 K) reflects the strikingly weak coupling between the fluctuating  $M$  and  $e_N$  in ferromagnets, compared with vortex flow in a superconductor [12, 15]. With the growth of long-range magnetic order below  $T_C$ , Eq. 3 ceases to be valid.

In the ferromagnetic state, we restrict our attention to the regime below 100 K where  $e_N^{\text{sat}}$  is nominally linear in  $T$ . Figure 3a shows curves in this regime for the 5 samples studied. The slopes of the low- $T$  curves are not monotonic in  $x$ . As  $x$  is increased from 0.1, the slope attains a maximum value at  $x = 0.25$ , and then decreases to a value close to its initial value when  $x$  reaches 1.0. This is perhaps unsurprising since  $e_N$  involves transport quantities  $S$ ,  $\rho$  and  $\rho_{xy}$  with opposite trends vs.  $x$ . By Eq. 1, we may find the curve of  $\alpha_{xy}$  vs.  $T$  by adding the curves  $e_N$  and  $S \tan \theta_H$  (Fig. 3b) and dividing by  $\rho$ . The data in Figs. 3a and 3b show that these terms are opposite in sign for  $x > 0.3$ . With increasing  $x$ , their mutual cancellation suppresses  $\alpha_{xy}$  strongly. In particular, at the largest  $x$  (0.85 and 1.0), the cancellation is nearly complete and  $\alpha_{xy}$  is very small below 100 K, i.e. the observed  $e_N$  is nearly entirely from the AHE of the backflow current. For  $0.1 \leq x < 0.3$ ,  $S \tan \theta_H$  is negligible and  $e_N$  largely reflects the behavior of  $\alpha_{xy}$ . We exclude from our study the undoped compound  $\text{CuCr}_2\text{Se}_4$  because  $e_N$  and  $\rho'_{xy}$  were not resolved at low  $T$ . These trends emphasize

the importance of knowing all 4 transport quantities, instead of just  $e_N$ , to discuss  $\mathbf{J}^Q$  meaningfully.

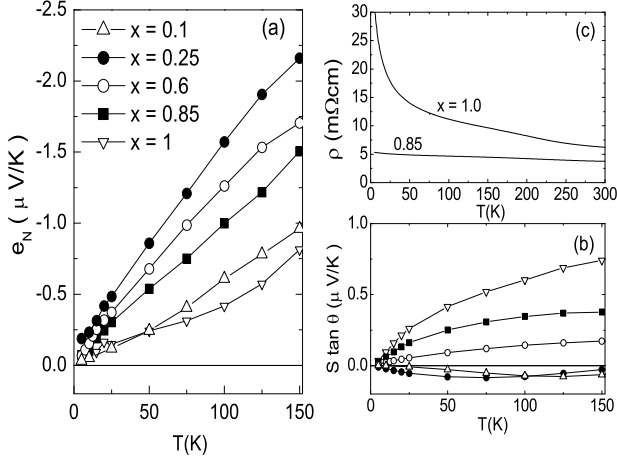


FIG. 3: (Panel a) Curves of  $e_N$  vs.  $T$  below 150 K in 5 samples with doping  $0.1 \leq x \leq 1.0$  showing nominal  $T$ -linear behavior at low  $T$ . The slopes vary non-monotonically with  $x$ . Panel (b) shows the Hall-current term  $S \tan \theta_H$  measured in the same samples. For  $x > 0.3$ ,  $S \tan \theta_H$  is opposite in sign from  $e_N$  [the symbol key applies to both (a) and (b)]. Panel (c) shows the sharp change in the  $\rho$ - $T$  profiles in the samples with  $x = 0.85$  and  $1.0$ . At low  $T$ ,  $\rho$  at  $0.85$  is metallic, but at  $1.0$ ,  $\rho$  reveals hopping between strongly localized states.

Finally, the derived curves of  $\alpha_{xy}$  vs.  $T$  are shown in Fig. 4. In contrast to the non-monotonic behavior of  $e_N$  vs.  $x$ ,  $\alpha_{xy}$  varies linearly with  $T$  as  $\alpha_{xy} = b(x)T + c$ , where the slope  $b(x)$  now decreases monotonically as  $x$  increases from  $0.1$  to  $1.0$  (Fig. 4). In all samples except  $x = 0.25$ , the parameter  $c$  – probably extrinsic in nature – is close to zero within our accuracy. The dependence of the parameter  $b(x) = [\alpha_{xy}(T) - \alpha_{xy}(0)]/T$  on these two quantities is of main interest. Figure 4b compares how  $b(x)$  and  $n_h$  – determined [8] from  $\rho_{xy}$  above  $T_C$  – vary with  $x$ . Whereas, at small  $x$ , the decrease in  $b(x)$  seems to match that of  $n_h$ ,  $b(x)$  falls much faster to zero at large  $x$ .

A striking relation between them becomes apparent if we plot one against the other. Figure 5 shows that, above a threshold doping near  $0.85$ ,  $b(x)$  increases as a fractional power of  $n_h - n_{h0}$  with  $n_{h0}$  a threshold density. This is consistent with  $b(x)$  increasing like the density of states (DOS), viz.  $b(x) \sim \mathcal{N}_F$ . The DOS for the free-electron gas  $\mathcal{N}_F^0$  (dashed curve) has a slightly stronger curvature than the data. Interestingly, the occurrence of the threshold doping at  $x = 0.85$  accounts well for a puzzling change in the resistivity behavior when  $x$  exceeds  $0.85$  (Fig. 3c). In general, slowly increasing  $x$  causes the resistivity profiles to change systematically, reflecting slight decreases in both  $n_h$  and  $\ell_0$  (mean-free-path). However, between  $0.85$  and  $1.0$ , the change is sudden and

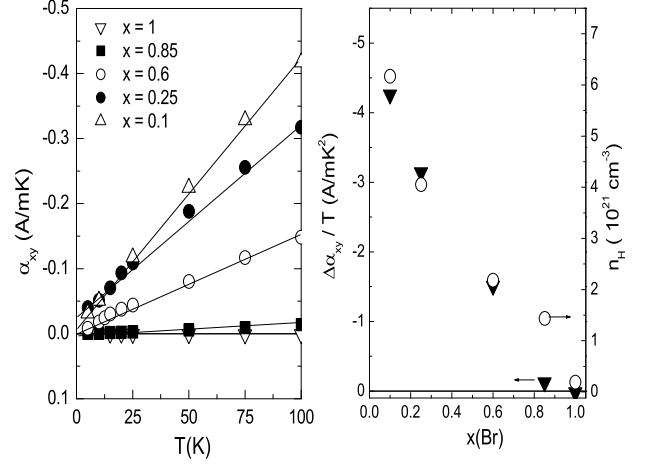


FIG. 4: [Panel (a)] Curves of  $\alpha_{xy}$  vs.  $T$  obtained by adding  $e_N$  and  $S \tan \theta_H$  (Eq. 1). The slope  $b(x)$  now falls monotonically as  $x$  increases to  $1.0$ . Panel (b) compares how the slope  $b(x) = \Delta\alpha_{xy}/T$  and  $n_h$  vary with  $x$ .

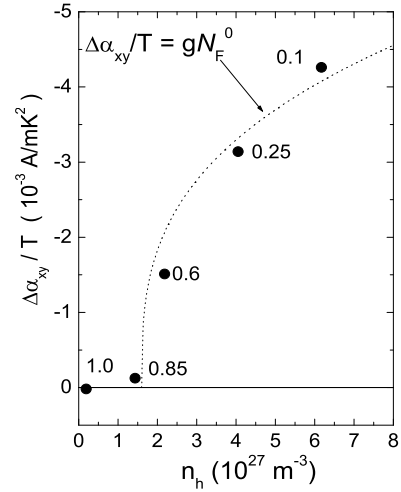


FIG. 5: Plot of  $b(x) = \Delta\alpha_{xy}/T$  against  $n_h$  showing that above the threshold doping ( $x \sim 0.85$ ),  $b(x)$  increases as a fractional power of  $n_h - n_{h0}$ . The dashed line is  $\Delta\alpha_{xy}/T = g\mathcal{N}_F^0$  with  $g = 9.77 \times 10^{-50}$  in SI units.

striking. At  $x = 0.85$ ,  $\rho$  is  $T$  independent below  $100$  K consistent with a disordered metal. By contrast, at  $1.0$ ,  $\rho$  rises monotonically with decreasing  $T$  (Fig. 3c). Between  $300$  and  $4.2$  K,  $\rho$  increases from  $6.3$  to  $32 \text{ m}\Omega\text{cm}$ . At low  $T$ , conductivity proceeds by hopping between strongly localized states in an impurity band. Figure 5 confirms that we reach the extremum of the hole band near  $x = 0.85$ . Further removal of carriers ( $x \rightarrow 1$ ) affects states within the impurity band.

Knowing  $n_h$  and  $\rho$  at each  $x$ , we may determine the mean-free-path  $\ell_0$  in the impurity-scattering regime. Between  $x = 0.1$  and  $1.0$ ,  $\ell_0$  decreases by a factor of 40. This steep decrease has no discernible influence on  $b(x)$ . Combining these factors then, we have  $\alpha_{xy} = gT\mathcal{N}_F$  where  $g$  is independent of  $\ell_0$ . We may boil down  $\alpha_{xy}$  to the measurement of an “area”  $\mathcal{A}$  by writing

$$\alpha_{xy} = \mathcal{A} \frac{ek_B^2 T}{\hbar} \mathcal{N}_F, \quad (T \ll T_C). \quad (4)$$

with  $k_B$  Boltzmann’s constant and  $e$  the electron charge. The value of  $g$  gives  $\mathcal{A} = 33.8 \text{ \AA}^2$  if we assume  $\mathcal{N}_F \sim \mathcal{N}_F^0$ . As the anomalous Hall heat current produced by  $\mathbf{E}||\hat{\mathbf{x}}$  is  $J_y^Q = \alpha_{yx}TE$ , it shares the simple form in Eq. 4. The ratio  $J_y^Q/J_y \sim T^2$ , as expected for a Fermi gas.

We briefly sketch the anomalous-velocity theory [2, 3, 4]. In a periodic lattice, the position operator for an electron is the sum  $\mathbf{x} = \mathbf{R} + \mathbf{X}(\mathbf{k})$  where  $\mathbf{R}$  locates a unit cell, while  $\mathbf{X}(\mathbf{k})$  locates the intracell position [16]. A finite  $\mathbf{X}(\mathbf{k})$  implies that  $\mathbf{x}$  does not commute with itself. Instead, we have [16]  $[x_j, x_k] = i\epsilon^{jkm}\Omega_m$  with  $\epsilon^{jkm}$  the antisymmetric tensor, which implies the uncertainty relation  $\Delta x_j \Delta x_k \sim \Omega$ . The ‘Berry curvature’  $\mathbf{\Omega}(\mathbf{k}) = \nabla_{\mathbf{k}} \times \mathbf{X}$  is analogous to a magnetic field in  $\mathbf{k}$  space [18]. In the presence of  $\mathbf{E}$ ,  $\mathbf{\Omega}$  adds a term that is the analog of the Lorentz force to the velocity  $\mathbf{v}_{\mathbf{k}}$ , viz.

$$\hbar \mathbf{v}_{\mathbf{k}} = \nabla \epsilon(\mathbf{k}) - \mathbf{E} \times \mathbf{\Omega}(\mathbf{k}). \quad (5)$$

The anomalous velocity term in Eq. 5 immediately implies the existence of a spontaneous Hall current  $\mathbf{J}_H = -2e \sum_{\mathbf{k}} f_{\mathbf{k}}^0 \mathbf{E} \times \mathbf{\Omega}(\mathbf{k})$  where  $f_{\mathbf{k}}^0$  is the unperturbed distribution [2, 3, 4, 7, 16]. The unconventional form of the current – notably the absence of any lifetime dependence – has made the KL theory controversial for decades [1, 19]. However, strong support has been obtained from measurements of Lee *et al.* [8] showing that the normalized AHE conductivity  $\sigma'_{xy}/n_h$  in  $\text{CuCr}_2\text{Se}_{4-x}\text{Br}_x$  is unchanged despite a 1,000-fold increase in  $\rho$ .

In general, the off-diagonal term  $\alpha_{xy}$  is related to the derivative of  $\sigma_{xy}$  at the chemical potential  $\mu$ , viz.  $\alpha_{xy} = \frac{\pi^2 k_B^2 T}{3e} \left[ \frac{\partial \sigma_{xy}}{\partial \epsilon} \right]_{\mu}$  [12]. Using the result [8] that  $\sigma'_{xy}$  is linear in  $n_h$  but independent of  $\ell_0$ , and  $[\partial n_h / \partial \epsilon]_{\mu} = \mathcal{N}_F$ , we see that  $\alpha_{xy} \sim T\mathcal{N}_F$ , consistent with Eq. 4. [By contrast, we note that the skew-scattering model [19] would predict  $\sigma'_{xy} \sim n_h \ell_0$  and  $\alpha_{xy} \sim T\mathcal{N}_F \ell_0$ .]

Finally,  $\mathcal{A}$  in Eq. 4 has the value  $34 \text{ \AA}^2$ . If Eq. 5 is indeed the origin of  $\alpha_{xy}$ ,  $\mathcal{A}$  must be roughly the scale of  $\Omega \sim \Delta x_j \Delta x_k$ . Hence the value  $\mathcal{A} \sim \frac{1}{3}$  the unit-cell area seems reasonable (the lattice spacing here is  $10.33 \text{ \AA}$ ). While a quantitative comparison requires knowledge of  $\mathbf{\Omega}(\mathbf{k})$  over the Brillouin zone, the simple form of Eq. 4 seems to provide valuable insight on the anomalous heat current.

A previous calculation of the Nernst coefficient was based on the “side-jump” model [17]. On scattering from an impurity, the carrier suffers a small sideways displacement  $\delta$  to give on average  $\tan \theta_H = \delta/\ell_0$ . This was used to derive  $Q_s \sim T(k_F \ell)^{-1}$ . In our experiment,  $k_F \ell$  falls monotonically, with increasing  $x$ , while  $e_N$  rises to a broad maximum near 0.25 before falling. Hence our experiment is in essential conflict with the side-jump model. From earlier experiments [11], an empirical form  $Q_s = -(a + b'\rho)T$  has been inferred ( $a, b'$  are constants). This is not borne out in our data.

Combining Nernst, Hall and thermopower experiments on the ferromagnet  $\text{CuCr}_2\text{Se}_{4-x}\text{Br}_x$ , we have determined how  $\alpha_{xy}$  (hence  $\mathbf{J}^Q$ ) changes as a function of  $n_h$  and  $\tau$ . At low  $T$ , we find that  $\alpha_{xy}$  follows the strikingly simple form  $\alpha_{xy} \sim \mathcal{A}T\mathcal{N}_F$ , consistent with the anomalous-velocity theory for the AHE (Fig. 4). In addition, a direct relation (Eq. 3) between  $M$  and  $\alpha_{xy}$  is observed in the paramagnetic regime above  $T_C$ .

We acknowledge support from the U.S. National Science Foundation (Grant DMR 0213706).

*\*Permanent address of S. W. : Center for Crystal Science and Technology, University of Yamanashi, 7 Miyamae, Kofu, Yamanashi 400-8511, Japan*

- 
- [1] For a review, see *The Hall Effect in Metals and Alloys*, ed. Colin Hurd (Plenum, New York 1972) p. 153.
  - [2] R. Karplus, J. M. Luttinger, Phys. Rev. **95**, 1154 (1954); J. M. Luttinger, Phys. Rev. **112**, 739 (1958).
  - [3] Ganesh Sundaram and Qian Niu, Phys. Rev. B **59**, 14915 (1999).
  - [4] M. Onoda, N. Nagaosa, J. Phys. Soc. Jpn. **71**, 19 (2002).
  - [5] S. Murakami, N. Nagaosa, S. C. Zhang, Science **301**, 1348 (2003).
  - [6] T. Jungwirth, Qian Niu, A. H. MacDonald, Phys. Rev. Lett. **88**, 207208 (2002).
  - [7] Yugui Yao *et al.*, Phys. Rev. Lett. **92**, 037204 (2004).
  - [8] Wei-Li Lee, Satoshi Watauchi, R. J. Cava and N. P. Ong, Science **303**, 1647 (2004).
  - [9] Alpheus W. Smith, Phys. Rev. **17**, 23-37 (1921); R. P. Ivanova. Fiz. metal. metalloved. **8**, 851-856 (1959).
  - [10] For a table of Nernst data, see *Handbook of physical quantities*, ed. Igor S. Grigoriev and Evgenii Z. Meilikhov, (Boca Raton, Fl., CRC Press, 1997), p. 904.
  - [11] E. I. Kondorskii, Sov. Phys. JETP **18**, 351 (1964); E. I. Kondorskii and R. P. Vasileva, Sov. Phys. JETP **18**, 277 (1964).
  - [12] Yayu Wang *et al.*, Phys. Rev. B **64**, 224519 (2001).
  - [13] K. Miyatani *et al.*, J. Phys. Chem. Solids **32**, 1429 (1971).
  - [14] In our convention, the sign of  $e_N$  is that of the Nernst signal of vortex flow in a superconductor [12], viz.  $e_N$  is positive if  $\mathbf{E}_N || \mathbf{H} \times (-\nabla T)$ .
  - [15] The value of  $\beta$  for vortex flow in superconductors is larger than in ferromagnets by  $\sim 10^5$  (see Eq. 3). This reflects a fundamental difference in how magnetization couples to

the Nernst signal in the 2 cases.

- [16] E. N. Adams, E. I. Blount, J. Phys. Chem. Solids **10**, 286 (1959).
- [17] L. Berger, Phys. Rev. B **2**, 4559 (1970); *ibid.* Phys. Rev. B **5**, 1862 (1972).
- [18] In terms of Bloch functions  $\psi_{n\mathbf{k}} = e^{i\mathbf{k}\cdot\mathbf{r}} u_{n\mathbf{k}}$ , the matrix element of the intracell operator  $\mathbf{X}(\mathbf{k}) = i \int d^3r u_{n\mathbf{k}}^* \nabla_{\mathbf{k}} u_{n\mathbf{k}}$  has the form of a Berry gauge potential whose line-integral gives a phase accumulation  $\gamma = \oint d\mathbf{k} \cdot \mathbf{X}(\mathbf{k})$  that reflects motion in an effective magnetic field  $\mathbf{\Omega} = \nabla_{\mathbf{k}} \times \mathbf{X}(\mathbf{k})$  existing in  $\mathbf{k}$  space.
- [19] J. Smit, Physica (Amsterdam) **21**, 877 (1955); *ibid.* Phys. Rev. B **8**, 2349 (1973).